Journal of Materials Chemistry

Cite this: J. Mater. Chem., 2011, 21, 7640

www.rsc.org/materials

PAPER

Ionic liquids and organic ionic plastic crystals utilizing small phosphonium cations

Vanessa Armel,[a] David Velayutham,†[ab] Jiazeng Sun,[a] Patrick C. Howlett,[ab] Maria Forsyth,[b] Douglas R. MacFarlane[a] and Jennifer M. Pringle*[ab]

Received 27th January 2011, Accepted 21st March 2011
DOI: 10.1039/c1jm10417a

The development of new liquid and solid state electrolytes is paramount for the advancement of electrochemical devices such as lithium batteries and solar cells. Ionic liquids have shown great promise in both these applications. Here we demonstrate the use of phosphonium cations with small alkyl chain substituents, in combination with a range of different anions, to produce a variety of new halide free ionic liquids that are fluid, conductive and with sufficient thermal stability for a range of electrochemical applications. Walden plot analysis of the new phosphonium ionic liquids shows that these can be classed as "good" ionic liquids, with low degrees of ion pairing and/or aggregation, and the lithium deposition and stripping from one of these ionic liquids has been demonstrated. Furthermore, for the first time phosphonium cations have been used to form a range of organic ionic plastic crystals. These materials can show significant ionic conductivity in the solid state and thus are of great interest as potential solid-state electrolyte materials.

Introduction

The use of ionic liquids is now prolific across many different areas of scientific research and commercialization. Their unique physicochemical properties impart excellent solubilising properties, hence their applicability for many different types of synthetic reactions, while their unparalleled electrochemical stability in some cases makes them highly advantageous as electrolytes for a wide range of electrochemical devices including dye-sensitized solar cells,[1,2] actuators[3–5] and batteries.[6–10] Ionic liquids have also attracted attention as green solvents for organic synthesis, catalysis and separations,[11–15] and are considered to be promising electrolytes for the electrodeposition of metals, alloys and nanomaterials.[16–19]

One of the many advantages of ionic liquids is that their physical properties can, to a certain extent, be tailored by judicious choice of the cation and anion. For example, the bis(trifluoromethanesulfonyl)amide anion (Fig. 1)[20] has been a champion anion for electrochemical applications; the electron withdrawing CF_3 group effectively delocalizes the negative charge across the anion, thereby reducing interactions with nearby cations. More recently, the smaller bis(fluorosulfonyl) amide anion (FSA, Fig. 1),[21–23] which also features significant charge delocalization, has been reported to impart even lower viscosities and higher conductivites,[24] however, some concerns have been raised about the stability of this anion at elevated temperatures.[25]

The range of cations commonly utilized in ionic liquids is less diverse than the choice of anion, with the vast majority of the research focusing on quaternary ammonium species such as the imidazolium, tetraalkyl ammonium or pyrrolidinium families.[13,26,27] Phosphonium cations have received less attention despite a number of distinct advantages in terms of stability[28,29]

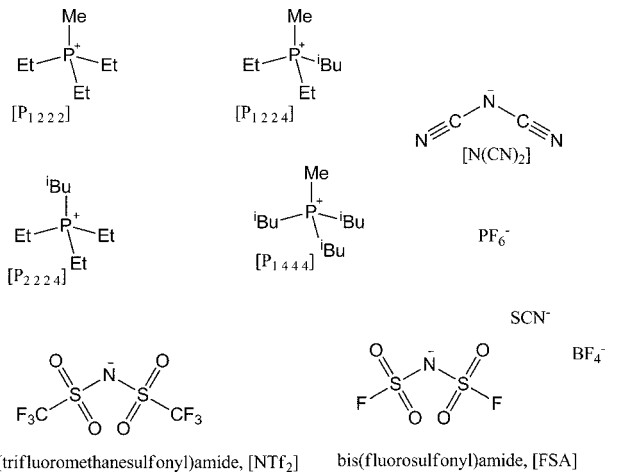

Fig. 1 The chemical structures, and abbreviations, of the cations and anions utilised in the new phosphonium-based ionic liquids and organic ionic plastic crystals.

[a]*School of Chemistry, Monash University, Clayton, VIC, 3800, Australia. E-mail: Jenny.Pringle@monash.edu*
[b]*Department of Materials Engineering, Monash University, Clayton, VIC, 3800, Australia*
† On deputation from the Central Electrochemical Research Institute (CSIR), Karaikudi-630006, India.

and the potentially enormous range of different salts that can be developed by modification of any of the four different alkyl substituents. A number of phosphonium ionic liquids are now commercially available,[28] but this still represents only a fraction of this large and promising family. Furthermore, the majority of research to-date has focused on phosphonium ionic liquids utilising large cations, such as the trihexyl(tetradecyl)phosphonium, [$P_{6\,6\,6\,14}$], which generally impart significantly higher viscosities, and hence lower conductivities, than the smaller species.[29] Thus, synthesis of ionic liquids utilising phosphonium cations with smaller alkyl chain substituents (and less symmetry where possible) is highly desirable for the development of these new ionic liquids for a range of different applications.

Applications of phosphonium ionic liquids currently include phase transfer catalysis,[30,31] in supercapacitors,[32] in dye-sensitised solar cells,[33–36] as corrosion inhibitors,[37–39] or lubricants,[40,41] and their improved suitability for use with strong bases, compared to that of the imidazolium-based ionic liquids, has been demonstrated.[42,43] Finally, their application in lithium batteries has been recognised.[44] However, despite the importance of such research, and the suitability of this type of ionic liquid for these devices, investigations into the electrochemical properties of phosphonium ionic liquids,[35,45,46] and the electrodeposition of lithium from these new materials,[47–49] are still sparse.

Organic ionic plastic crystals are crystalline phases found in many of the same organic salt families that exhibit various forms of disorder and therefore exhibit plastic mechanical properties.[50] This, and their intrinsic ionic conductivity, makes them of interest as solid state ion conductors.[51,52] The plastic phase is typically reached by one or more solid–solid phase transitions on warming of the fully ordered crystalline phase from low temperatures. Interestingly, there has been little attention paid thus far to the occurrence and properties of this type of phase behaviour in the phosphonium family of organic salts.

Here we report the synthesis of novel, halide free phosphonium salts utilising small cations with a range of different anions (Fig. 1). While use of the bis(trifluoromethane)sulfonyl amide and bis(fluorosulfonyl)amide anions allows the formation of a number of novel ionic liquids, use of the hexafluorophosphate, tetrafluoroborate or thiocyanate anions also allows the synthesis of new organic ionic plastic crystals, which are of significant interest in a number of applications of solid state electrolytes. Further, the electrochemical stability and efficacy of lithium deposition from the new phosphonium ionic liquids are demonstrated using both alloying and non-alloying electrodes.

Results and discussion

For a large number of synthetic and electrochemical applications, the presence of halides in an ionic liquid can have a detrimental, even catastrophic, effect.[53] Furthermore, the presence of even low levels of halide impurities can significantly reduce the window of electrochemical stability,[54] thus limiting their applicability in electrochemical devices. Among the phosphonium salts commercially available, those utilising the tosylate anion have the added advantage that they can be synthesised halide free, by direct reaction of the tertiary phosphine with an alkyl tosylate, without the need to generate the tetraalkylphosphonium halide intermediates.[28] Thus, utilisation of phosphonium tosylate salts as starting materials then allows the facile metathesis into a range of alternative salts, according to eqn (1), to allow the formation of a range of halide free phosphonium salts.

$$[R'R''\ PR_2]^+[Tos]^- + MA \rightarrow [R'R''\ PR_2]^+[A]^- + M\text{Tos} \quad (1)$$

where M = Li, Na, K; A = NTf_2, FSA, PF_6, BF_4, SCN and R, R', R'' = Me, Et, ^{i}Bu.

Thermal properties

The new ionic liquids show diverse thermal properties depending on the structure of the cation and the anion, as shown in Fig. 2. The phase transition temperature data and the entropies of fusion (ΔS_f) are summarised in Table 1. A low entropy of melting is a well known characteristic of plastic crystal behaviour; typically well ordered crystalline organic salts can have $\Delta S_f > 60$ J mol^{-1} K^{-1}, while the disorder present in the plastic phase can lower ΔS_f to less than 20 J K^{-1} mol^{-1}.[55] The salts have been classified according to the traditional definition,[56] where those with a melting point of below 100 °C are considered to be ionic liquids. Those with melting points above 100 °C, and that display at least one solid–solid phase transition, fall into the category of organic ionic plastic crystals and these are discussed in the next section. However, there are a number of new phosphonium salts reported here that have melting points above room temperature but below 100 °C and that also display plastic crystal behaviour, such as multiple solid–solid phase transitions and low entropies of melting, and hence we have also considered these materials as organic ionic plastic crystals. Thus, it is important to note that there is some overlap between the two families, and that the classification depends to a certain extent on the use; an organic ionic plastic crystal with a melting point above room temperature may be useful as a solid state electrolyte in electrochemical devices, but may also be used as an ionic liquid in higher temperature applications.

For completeness, the $N(CN)_2$ salt of the [$P_{1\,2\,2\,4}$] cation is discussed within the family of new phosphonium ionic liquids. However, in parallel with our work, the $N(CN)_2$ salts of the [$P_{1\,4\,4\,4}$] and [$P_{2\,2\,2\,4}$] cations have recently been reported,[45] and hence, although we also prepared these salts, they are not further

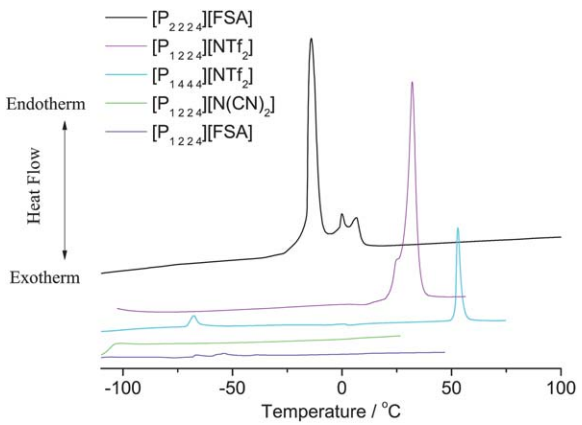

Fig. 2 The thermal behaviour of the phosphonium ionic liquids.

Table 1 The thermal behaviour of the new phosphonium ionic liquids, as determined by differential scanning calorimetry

	Phase transition				
	II–I		I–Melt		
	$T \pm 1$/°C	$\Delta S \pm 5\%$ (J mol^{-1} K^{-1})	$T \pm 1$/°C	$\Delta S_f \pm 5\%$ (J mol^{-1} K^{-1})	Decomposition temp/°C
$[P_{2\,2\,2\,4}][FSA]$	−16	46	*ca.* 4	6	250
$[P_{1\,2\,2\,4}][NTf_2]$			28	50	300
$[P_{1\,4\,4\,4}][NTf_2]$	−68	19	52	59	330
$[P_{1\,2\,2\,4}][N(CN)_2]$			$T_g = -106$ °C		320
$[P_{1\,2\,2\,4}][FSA]^a$			*ca.* −55 °C		250

[a] As $[P_{1\,2\,2\,4}][FSA]$ has such a low entropy of fusion, quenching was performed to visually confirm crystallisation; upon cooling the sample to −80 °C a white solid formed, indicating crystallisation.

discussed here. The melting point of $[P_{1\,2\,2\,4}][NTf_2]$ has also been reported,[46] but no other properties were given and thus discussion of this salt is included.

Examination of the thermal properties of the new ionic liquids shows that the FSA anion imparts lower melting points than the NTf_2 anion; for example $[P_{1\,2\,2\,4}][FSA]$ melts about 80 °C below $[P_{1\,2\,2\,4}][NTf_2]$. A decrease in the length of the alkyl chain substituent also produces a consistent decrease in melting point; the melting point of $[P_{1\,2\,2\,4}][FSA]$ is more than 50 °C below that of $[P_{2\,2\,2\,4}][FSA]$. Finally, although $[P_{1\,4\,4\,4}][NTf_2]$ displays a small solid–solid phase transition at −68 °C before melting at 52 °C, the entropy of fusion is still large (59 J mol^{-1} K^{-1}) and therefore this compound does not appear to be exhibiting strong plastic crystalline behaviour.

Molecular plastic crystals, such as succinonitrile, were first described in the 1960s,[55] and this early work identified a number of features of plastic crystal behavior, such as the low entropy of melting. As the most plastic phase of these compounds is commonly reached *via* one or more solid–solid phase transitions, which represent the onset of molecular rotations within the material, the rotational component of the entropy of fusion is already present in the solid phases and hence the entropy of fusion in the transition from phase I to the melt is small (by convention, the highest temperature solid phase is denoted phase I, with subsequent lower temperature phases denoted phase II, III, *etc.*). In other words, by phase I the material can be quite disordered and "liquid like". However, this criterion may only be appropriate to plastic crystals containing one molecular species; if the plastic crystal contains two different ions, as is the case for organic ionic plastic crystals, and only one of the ions exhibits rotator motions, then the entropy of melting may be higher than 20 kJ mol^{-1}, as is observed for a number of organic ionic plastic crystals,[57] including some of the phosphonium salts reported here.

A number of the new phosphonium salts synthesised display high melting points and multiple solid–solid phase transitions (Fig. 3 and Table 2). This is of significant interest as it is the first observation of organic ionic plastic crystals utilising phosphonium cations.

The $[P_{1\,2\,2\,4}]$ cation forms plastic crystals when combined with the SCN, BF_4 and PF_6 anions; these materials melt at lower temperatures than their $[P_{1\,4\,4\,4}]$ analogues, but at temperatures that are still sufficiently high for their potential application as solid state electrolytes for a range of electrochemical devices.

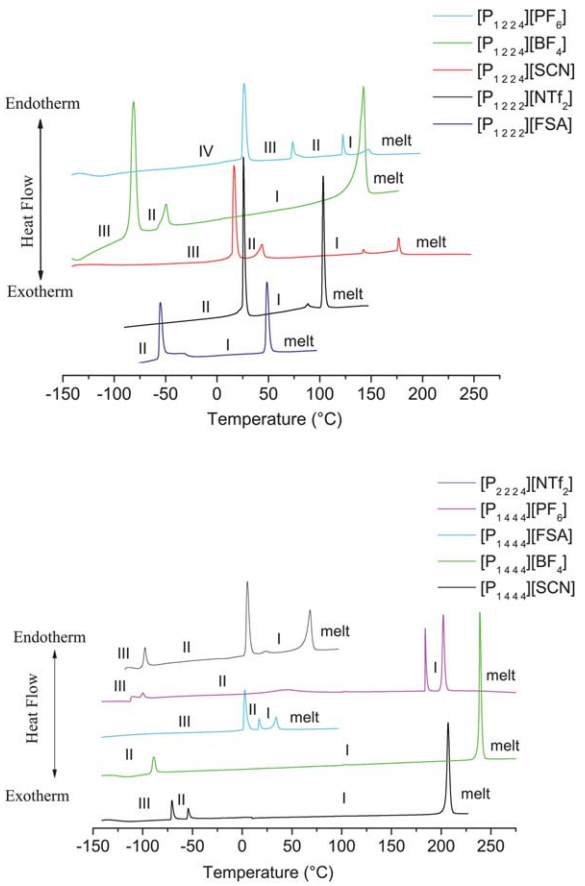

Fig. 3 The thermal behaviour of the new organic ionic plastic crystals with small phosphonium cations.

All of these salts show rich phase behaviour, with multiple solid–solid phase transitions, while the entropy of fusion of the $[P_{1\,2\,2\,4}][PF_6]$ and $[P_{1\,2\,2\,4}][SCN]$ salts is extremely small—the smallest that we have previously observed for any organic ionic plastic crystal—indicating that the materials are very disordered in phase I. This is consistent with the high conductivity of these salts, as discussed further below. The thermal behaviour of the SCN and BF_4 salts, which are in phase I over a relatively wide and suitable temperature range, is also ideal for their use as solid state electrolytes.

Table 2 The thermal behaviour of the new phosphonium organic ionic plastic crystals, as determined by differential scanning calorimetry

	Phase transition								
	IV–III		III–II		II–I		I–Melt		
	$T \pm 1$/°C	$\Delta S \pm 5\%$ (J mol^{-1} K^{-1})	$T \pm 1$/°C	$\Delta S \pm 5\%$ (J mol^{-1} K^{-1})	$T \pm 1$/°C	$\Delta S_f \pm 5\%$ (J mol^{-1} K^{-1})	$T \pm 1$/°C	$\Delta S_f \pm 5\%$ (J mol^{-1} K^{-1})	Decomposition temp/°C
$[P_{1\,2\,2\,4}][PF_6]$	24	39	72	6	122	4	139	3	270
$[P_{1\,2\,2\,4}][BF_4]$			−85	34	−55	5	136	19	300
$[P_{1\,2\,2\,4}][SCN]$[a]			15	33	38	7	176	2	295
$[P_{1\,2\,2\,2}][NTf_2]$					25	38	102	26	320
$[P_{1\,2\,2\,2}][FSA]$					−55	27	47	23	220
$[P_{2\,2\,2\,4}][NTf_2]$			−100	10	3	25	63	20	350
$[P_{1\,4\,4\,4}][PF_6]$			−100	3	184	8	202	18	308
$[P_{1\,4\,4\,4}][FSA]$			7	46	24	9	36	23	220
$[P_{1\,4\,4\,4}][BF_4]$					−89	32	239	45	310
$[P_{1\,4\,4\,4}][SCN]$			−71	13	−51	8	207	44	300

[a] The small peak before the melt, at 141 °C, is considered to be too small to be classed as a solid–solid phase change.

The $[P_{1\,2\,2\,2}]$ cation forms plastic crystals with both the FSA and NTf_2 anions, although, consistent with the behaviour observed for the ionic liquids, the FSA salt is significantly lower melting (47 °C) than the NTf_2 (102 °C). Interestingly, the $[P_{1\,2\,2\,2}][NTf_2]$ melts at a higher temperature than the larger $[P_{2\,2\,2\,4}][NTf_2]$ salt, which may be a result of the smaller cation allowing more efficient packing and highlights the difficulty in predicting such physico-chemical relationships.

The DSC trace of $[P_{1\,4\,4\,4}][PF_6]$ shows evidence of three phase transitions over the temperature range studied; the first solid–solid phase transition appears as a combination of two peaks at −100 °C, the phase II → I transition appears as a sharp peak at 184 °C, before a final melting transition at 202 °C. The entropy of fusion (ΔS_f) of the $[P_{1\,4\,4\,4}][PF_6]$ is 18 J mol^{-1} K^{-1}, which is within Timmermans' criteria for a plastic crystal,[55] and indicates that the material is relatively disordered in phase I.

Both $[P_{1\,4\,4\,4}][BF_4]$ and $[P_{1\,4\,4\,4}][SCN]$ are in phase I over a very wide (>250 °C) temperature range; as this is the most conductive phase, this is a highly beneficial attribute for any plastic crystal with potential applications as a solid state electrolyte for electrochemical devices. However, the entropy of fusion of these compounds are relatively large, and hence outside the criteria for molecular plastic crystals,[55] which suggests that in phase I the materials are not completely rotationally disordered. This is also reflected in the low conductivities of these salts compared to their $[P_{1\,2\,2\,4}]$ analogues, as discussed later.

Thermal stability

Many of the potential applications of ionic liquids centre on their ability to be used at high temperatures without degradation; their use as replacements for traditional organic solvents relies on the ability to remove solvents and reagents/products by distillation at elevated temperatures, while recycling of the ionic liquid, which is crucial to overcome cost disadvantages, may also require exposure to high temperatures. Furthermore, the potential use of ionic liquids in applications such as catalysis, in high temperature electrodeposition processes or in electrochemical devices that may be exposed to elevated temperatures over extended time periods makes their thermal stability of critical importance. Thermogravimetric analysis of the new phosphonium ionic liquids (Fig. 4) clearly indicates that, across the range of different cations studied, the NTf_2 anion imparts superior thermal stability compared to the FSA anion. This is consistent with recent studies on FSA ionic liquids utilizing imidazolium and pyrrolidinium cations,[25,58] which raise concern over the suitability of these electrolytes for some applications. The traces also suggest a difference in the decomposition mechanism of the two types of materials as only the FSA salts show two or three different stages of decomposition.

The thermal stability of the new phosphonium salts with the BF_4, PF_6, SCN and $N(CN)_2$ anions (Tables 1 and 2) ranges from 270 °C for $[P_{1\,2\,2\,4}][PF_6]$ to 320 °C for $[P_{1\,2\,2\,4}][N(CN)_2]$, which is sufficient for many applications.

Viscosity

The viscosity of an electrolyte can significantly limit the performance of electrochemical devices as it influences the ionic conductivity and mass transport of ionic species through the electrolyte. The viscosity of ionic liquids depends strongly on temperature, as shown in Fig. 5 and Table 3, for the phosphonium salts analysed. As is often observed for ionic liquids, the temperature dependence of the viscosity shows a slight deviation from Arrhenius behaviour in the lower temperature region, as indicated by the non-linearity of the plots.

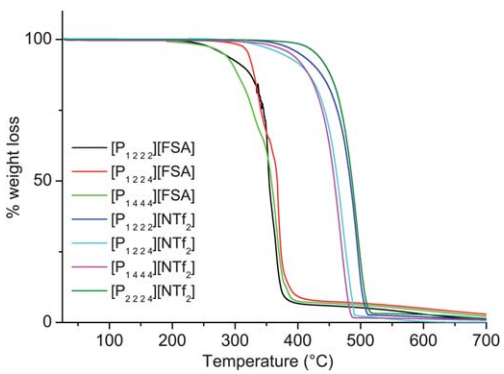

Fig. 4 Thermogravimetric analysis traces of the FSA and NTf_2 phosphonium salts.

The nature of both the anion and the cation can significantly influence the viscosity of an ionic liquids, but utilisation of the smaller $[P_{1\,2\,2\,4}]$ cation successfully produces relatively fluid ionic liquids with the FSA, NTf_2 and $N(CN)_2$ anions, with little difference between the salts. In contrast, the use of the larger $[P_{1\,4\,4\,4}]$ cation results in an increase in viscosity with both the NTf_2 and FSA anions.

Measurement of the densities of the different phosphonium ionic liquids (Table 3) shows that the fluorinated anions result in denser ionic liquids than for the dicyanamide-based species, which has a density similar to water.

Conductivity

Clearly one of the most fundamental attributes of any electrolyte is the conductivity, and in ionic liquids and organic ionic plastic crystals this can be heavily influenced by the nature of the cations and anions. The ionic conductivity of a pure ionic liquid depends on the mobility of ions, which is influenced by the size of the ion, the formation of any aggregated species, and the viscosity. The high temperature conductivities of the new phosphonium ionic liquids (Fig. 6a) are similar for salts utilising the $[P_{1\,2\,2\,4}]$ cation, and slightly lower for the larger $[P_{1\,4\,4\,4}]$ ionic liquid. The conductivity of the$[P_{1\,2\,2\,4}][FSA]$ and $[P_{1\,2\,2\,4}][N(CN)_2]$ salts at room temperature are 4.3 mS cm^{-1} and 3.8 mS cm^{-1}, respectively, while at 30 °C the conductivity of $[P_{1\,2\,2\,4}][NTf_2]$ is 3.2 mS cm^{-1}. This is an increase in conductivity compared to the longer chained species; the conductivity of $[P_{2\,2\,2\,8}][NTf_2]$ is 0.98 mS cm^{-1} at 25 °C,[46] whereas the conductivity of $[P_{2\,2\,2\,8}][N(CN)_2]$ is 2.0 mS cm^{-1} at 25 °C.[45]

The significant differences in conductivity of the different salts at lower temperatures (Fig. 6a) are a result of the different thermal behaviours, *i.e.* melting points. For example, $[P_{1\,4\,4\,4}][NTf_2]$, which melts at 52 °C, shows low conductivity in the low temperature region but this increases steadily as the temperature increases towards the melt. Interestingly, although there is no ambient temperature phase change visible in the DSC of this material (Fig. 2), there is a significant (reproducible) increase in the solid state conductivity at 25 °C, similar to the steps in conductivity previously observed at the phase changes of other organic ionic plastic crystals,[59,60] which may suggest an increase in the disorder or a change in the conductivity mechanism within the material at this temperature. As the temperature is further increased, the subsequent significant conductivity increase is a result of the salt melting, and a similar jump in the conductivity is observed upon the melting of $[P_{2\,2\,2\,4}][NTf_2]$, at 63 °C (Fig. 6a).

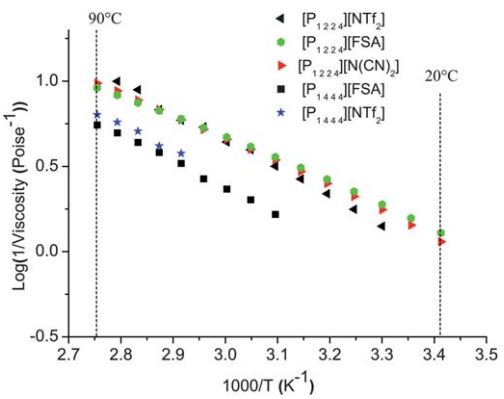

Fig. 5 The viscosity of the low-melting phosphonium salts.

Table 3 The room temperature densities and viscosities of the new phosphonium salts

	Viscosity ± 0.1/mPa s	Density ± 0.01/g cm^{-3}
$[P_{1\,2\,2\,4}][FSA]$	64	1.38
$[P_{1\,2\,2\,4}][NTf_2]$	72[a]	1.40[a]
$[P_{1\,2\,2\,4}][N(CN)_2]$	69	1.01
$[P_{1\,4\,4\,4}][FSA]$	30[b]	1.14[b]
$[P_{1\,4\,4\,4}][NTf_2]$	27[b]	1.23[b]

[a] Measured at 30 °C. [b] Measured at 70 °C.

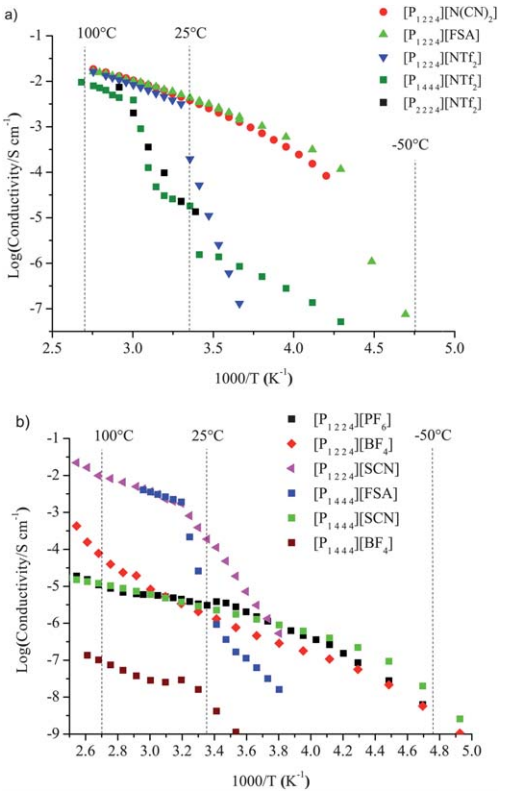

Fig. 6 The ionic conductivity of (a) the new phosphonium ionic liquids and (b) the phosphonium organic ionic plastic crystals.

The solid state conductivities of the new phosphonium-based organic ionic plastic crystals are also heavily influenced by the nature of the cation and anion and by the thermal behaviour of the different salts. The conductivity of $[P_{1\,2\,2\,4}][PF_6]$ increases steadily until the phase IV to III transition, at 24 °C, but remains relatively constant through the III to II transition and only starts to increase significantly at temperatures above 100 °C, which is approaching the phase II to I transition (122 °C) and the melt (139 °C, Table 2). The conductivity of $[P_{1\,2\,2\,4}][BF_4]$ increases slowly up until room temperature and then at an increased rate at higher temperatures; this change in gradient is not associated with any phase change in the material, which is in phase I between −55 °C and 136 °C (Table 2). In a similar vein, although the phase behaviour of $[P_{1\,4\,4\,4}][SCN]$ and $[P_{1\,2\,2\,4}][PF_6]$ is

markedly different (Fig. 3), these materials exhibit similar temperature-dependent conductivities, illustrating the complexity of predicting the ionic conductivities of these systems.

The conductivity of $[P_{1\ 4\ 4\ 4}][BF_4]$ is perhaps lower than expected considering that this material is in phase I across this temperature range, but it should be noted that the entropy of fusion is relatively high (45 J mol^{-1} K^{-1}) and therefore the material is not particularly disordered. For the ultimate solid state conductivity, it is most beneficial for an organic ionic plastic crystal to be as entropically close to the liquid state as possible. Nevertheless, while the conductivity of $[P_{1\ 4\ 4\ 4}][BF_4]$ is prohibitively low for use of the material as a solid state electrolyte in its neat state, the addition of a second ionic component as a dopant, or the addition of inorganic nanoparticles, may increase the conductivity to more practically useful levels.[50,52]

$[P_{1\ 4\ 4\ 4}][FSA]$ has two solid-solid phase transitions immediately before the melt at 36 °C, which is reflected in the rapid increase in conductivity in this region. Remarkably, the conductivity of $[P_{1\ 2\ 2\ 4}][SCN]$ in the solid state, in phase I, is very similar to that of *molten* $[P_{1\ 4\ 4\ 4}][FSA]$! (1.75×10^{-3} S cm^{-1} at 40 °C.) It is this fast ion conduction that makes the use of these materials as solid state electrolytes so compelling.

Ionicity

The product of ionic mobility and solvent viscosity, known as the Walden product,[61,62] can provide valuable insight into the degree of ionic interactions within an ionic liquid.[63] For infinitely dilute electrolyte solutions, the Walden product is a constant expressed by $\Lambda\eta = k$, where Λ is the molar conductivity, η is the viscosity and k is a temperature-dependent constant. Thus, this predicts that a plot of log Λ *vs.* log $1/\eta$ gives a straight line that passes through the origin; the "Walden plot". Assessment of this relationship for ionic liquids compared to the behaviour of a completely dissociated reference material—provided by data from a 0.01 M KCl solution, which provide the so-called "ideal line"—allows qualitative assessment of ion association such that any downward deviation from the ideal line indicates the presence of ion pairing, aggregation or the low dissociation of ions.[61] Indeed, Angell *et al.*[61] have classified the behaviour of ionic liquids, according to the Walden rule, into different categories: superionic (above the line), poor (at least an order of magnitude below the line) or good (close to the line). For example, protic ionic liquids generally fall well below the line, due to incomplete proton transfer, and are thus considered to be poor ionic liquids.[62,64]

The Walden plot of the new phosphonium ionic liquids (Fig. 7) shows that the salts all lie slightly below the ideal line, indicating that they have a low degree of pairing or aggregation type interactions and that they can therefore be considered as "good" ionic liquids. It appears therefore that the previously observed tendency of some phosphonium ionic liquids to exhibit ion association is a tendency of the larger phosphonium cations that were involved in that work.[63]

Electrochemical properties

The electrochemical stability of an ionic liquid is paramount for its successful use as an electrolyte in electrochemical applications such as lithium batteries. Lithium ion batteries commonly utilise a lithium conducting liquid or solid electrolyte, where a lithium salt such as $LiNTf_2$ is dissolved in a mixture of organic solvents, for example cyclic carbonates.[8] However, ionic liquids have recently attracted significant attention as electrolytes for lithium batteries because of their non-flammability, thermal stability, high ionic conductivity and wide electrochemical window.[9,65,66] At least 4 V of electrochemical stability is necessary for any lithium-ion conducting electrolyte to be used in this context. For this application, ionic liquids utilising the imidazolium cation have been the most widely studied,[8] but the use of alternative ammonium-based cations, such as quaternary ammoniums, pyrrolidiniums, morpholiniums, *etc.* has also been reported.[6–10] Recently, interest has turned to the use of quaternary phosphonium ionic liquids as electrolytes for electrochemical devices, because of their enhanced thermal stability, low viscosity and high ionic conductivity.[45,46,67] However, there is still a scarcity of studies on the electrochemistry of these materials,[10,46] and even fewer that report the electro-deposition of lithium.[47–49] This is the first study of lithium deposition and stripping from ionic liquids utilising a small phosphonium cation.

The cyclic voltammograms of $[P_{1\ 2\ 2\ 4}][NTf_2]$ and $[P_{1\ 4\ 4\ 4}][NTf_2]$ are shown in Fig. 8; these ionic liquids show electrochemical windows approaching 6 V, with anodic and cathodic limiting potentials up to 3.0 and −3.0 V respectively. Close examination of the cyclic voltammograms reveals a small anodic peak current at around 1 V, which is the result of the re-oxidation of reduced components in the ionic liquids, as observed in earlier work.[68,69] To verify this, the anodic and cathodic limiting potentials of $[P_{1\ 2\ 2\ 4}][NTf_2]$ were recorded separately using a freshly polished glassy carbon electrode (Fig. 8b and c), and these scans showed no peak at 1 V.

Generally, it is the cation of the ionic liquid that most influences the cathodic stability limit, and the anion that influences the anodic limit, although the anion can also limit the cathodic stability.[10] Interestingly, comparison of the two different phosphonium ionic liquids (Fig. 8a) shows that the while the cathodic stability of the two ionic liquids is the same, the $[P_{1\ 2\ 2\ 4}]$ cation imparts a slightly better anodic stability than the $[P_{1\ 4\ 4\ 4}]$ when combined with the same anion. Thus, this ionic liquid was chosen for the lithium electrodeposition-stripping studies.

Cyclic voltammograms in the lithium deposition and stripping region of potential on the glassy carbon electrode are shown in Fig. 9a. A well defined cathodic deposition peak is observed in

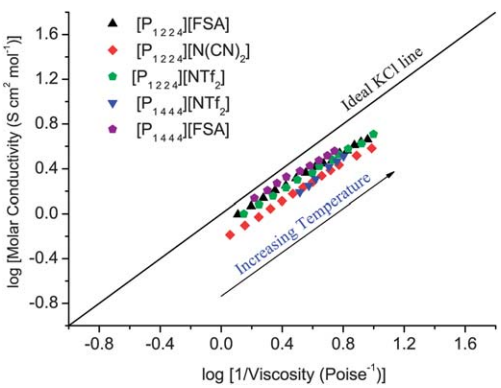

Fig. 7 The Walden plot of the new phosphonium ionic liquids.

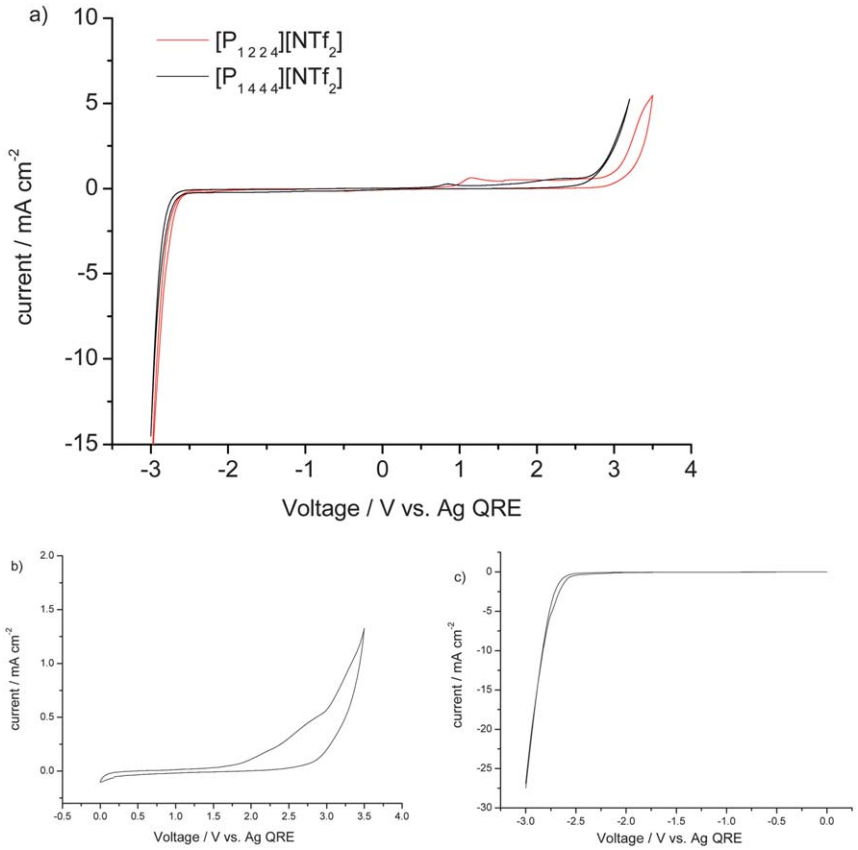

Fig. 8 a) Cyclic voltammograms of $[P_{1\,2\,2\,4}][NTf_2]$ and $[P_{1\,4\,4\,4}][NTf_2]$, at 50 °C and 90 °C, respectively, on a glassy carbon working electrode, (b) anodic potential limit of $[P_{1\,2\,2\,4}][NTf_2]$ at 50 °C, and (c) cathodic potential limit of $[P_{1\,2\,2\,4}][NTf_2]$ at 50 °C. Scan rate: 50 mV s^{-1}.

the first scan but with subsequent sweeps the deposition shifts to more negative potentials and the current decreases considerably. No stripping peak is visible in the reverse scan. At slower sweep rates (10 mV s^{-1}, Fig. 9b) some nucleation and growth of metallic lithium is perhaps evident, and the deposition current increases slightly with cycle number as the surface area during the nucleation process increases. The absence of an oxidation peak and the very small stripping currents on the glassy carbon electrode suggest the formation of a thick solid electrolyte interphase SEI layer due to the breakdown of the ionic liquid, which influences the lithium deposition–stripping and may restrain the lithium redox behaviour.[70] It further suggests a role for the native oxide film on the metal electrode as well as the underpotential deposition processes known to occur on a Pt electrode.[71]

The cyclic voltammograms of lithium deposition and stripping, on a nickel electrode, are shown in Fig. 9c. The sharp rise in the cathodic current at −0.2 V *vs.* Li/Li^+ is characteristic of the reduction of lithium ions to metallic lithium, with the anodic peak at 0.1 V in the reverse scan corresponding to the subsequent oxidation of the deposited lithium metal. The lithium deposition current decreases with cycle number, and the stripping peak moves towards more positive potentials, suggesting the formation of solid electrolyte interphase films, probably involving the IL, which in this case is able to support lithium transport through the film.[8,10,72] The broad pre-peak at around 0.35 V in the first cycle is related to SEI formation from the $[NTf_2]$ anion, particularly when a small quantity of water is present in the IL,[73,74] and the under-potential deposition of lithium may also occur at these potentials.[10,49] The "cross-over loop", obtained between the cathodic and anodic parts of the voltammograms during the reverse scan, is characteristic of a nucleation and growth process occurring during the electrodeposition of lithium.[6,17,18,69]

On platinum, bulk lithium deposition starts around 0 V *vs.* Li/Li^+ (Fig. 9d) and multiple stripping peaks occur during the reverse scan, characteristic of the formation of a Li–Pt alloy.[7,8,10,75] The lithium deposition shifts to more negative potentials with increasing cycle number, while the stripping shifts to more positive potentials, and the corresponding current decreases. This behaviour is attributed to the deposition of 'mossy' lithium, under the diffusion limited conditions in the CV experiment, and subsequent 'fouling' of the electrode surface. Comparison of the lithium stripping peaks from the Pt electrode (Fig. 9d) with those of the nickel (Fig. 9c) suggests that the peak common to both, at around 0.25 V, is due to the stripping of metallic lithium, while the other peaks that occur with the Pt electrode are a result of Li–Pt alloys.[7,8,10,75]

Conclusions

In the drive towards expanding the range of useful ionic liquids, with suitably low viscosities and sufficient stability and

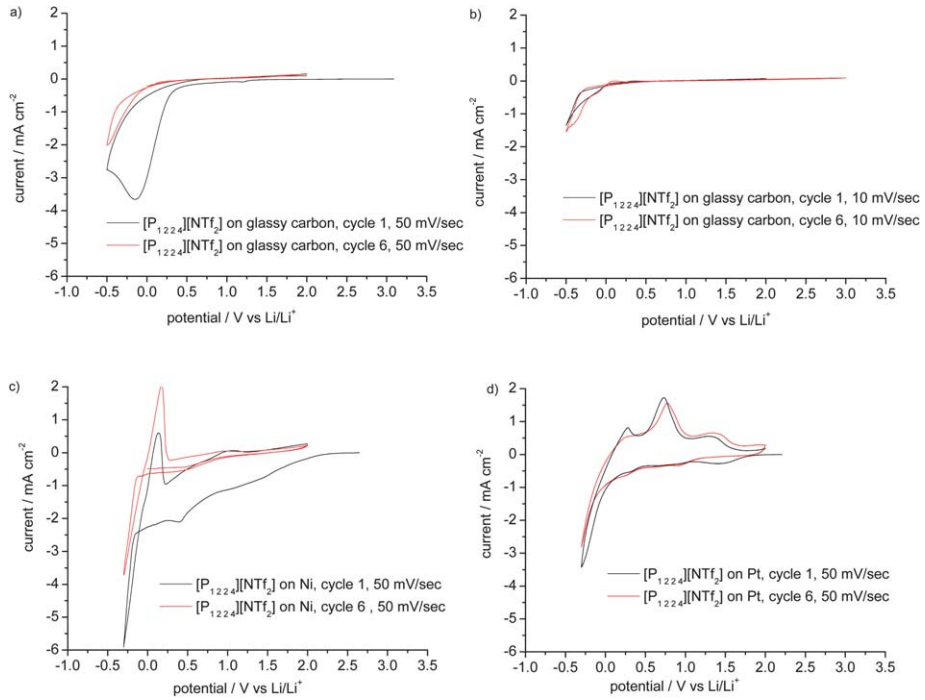

Fig. 9 Cyclic voltammograms of lithium deposition/stripping, on different working electrodes, from $[P_{1\,2\,2\,4}][NTf_2]$ with $LiNTf_2$ (0.2916 mol kg^{-1}), at 50 °C: (a) glassy carbon, scan rate 50 mV s^{-1}, (b) glass carbon, scan rate 10 mV s^{-1}, (c) Ni, scan rate 50 mV s^{-1}, and (d) Pt, scan rate 50 mV s^{-1}.

conductivity for electrochemical uses, phosphonium-based ionic liquids are proving exceptionally promising. Utilisation of smaller alkyl groups on the phosphonium cation, in combination with a range of different anions, yields a variety of new ionic liquids and organic ionic plastic crystals that are very promising electrolyte materials for both solid- and liquid-state devices. The ability to synthesise these salts halide free, through the tosylate intermediate, is an added advantage, particularly for electrochemical applications where residual halide impurities in ionic liquids is a continuing problem. Walden plot analysis of the new phosphonium ionic liquids shows that these can be classed as "good" ionic liquids, with low amounts of the ion pairing and/or aggregation that can be detrimental to the viscosity and conductivity. Furthermore, initial results indicate the electrochemical stability of the salts to be good, and the successful deposition and stripping of lithium ions has been demonstrated.

Experimental

Analysis

The purity of the ionic liquids was confirmed by NMR, Electrospray Mass Spectroscopy and Karl Fischer (for water content). *No trace of the tosylate anion was observed in any of the NMR or mass spectra*. Differential scanning calorimetry was performed across the temperature range of −150 °C to 250 °C, at a scan rate of 10 °C min^{-1}. Transition temperatures were reported using the peak maximum of the thermal transition and entropies of fusion were calculated from the melting endotherm area (ΔH_f) according to $\Delta S = \Delta H_f/T_m$.

Thermogravimetric analysis was performed using a dry nitrogen atmosphere, at a heating rate of 10 °C min^{-1} in platinum pans.

Density measurements were performed using an Anton Paar DMA 5000 density meter, from room temperature to 90 °C. The viscosity was measured using an Anton Paar AMVn, from room temperature to 90 °C. The viscosity of $[P_{1\,2\,2\,4}][FSA]$ and $[P_{1\,2\,2\,4}][N(CN)_2]$ was measured from 25 °C to 90 °C, while $[P_{1\,4\,4\,4}][FSA]$ was measured from 40 °C to 90 °C and $[P_{1\,2\,2\,4}][NTf_2]$ was measured from 30 °C to 90 °C as these latter salts are solids at room temperature. The viscosity of $[P_{1\,4\,4\,4}][NTf_2]$ could only be recorded above 60 °C as the melting point of the salt is 52 °C.

Cyclic voltammetry was performed using a Princeton Applied Research VMP2/Z multi-channel potentiostat and EC-Lab® software v9.55 using a three electrode cell system. The electrochemical window of the ionic liquid was measured using a 1 mm diameter glassy carbon disc as a working electrode, coiled platinum wire as the counter electrode and a silver wire quasi-reference electrode at 50 °C. A Ag wire pseudo reference was used to allow initial comparative assessment of the width of the electrochemical window and any intermediate processes. The glassy carbon electrode was polished using 0.05 μm alumina, washed thoroughly with distilled water and dried under a nitrogen stream. The ionic liquids were dried under vacuum at 70 °C for 24 h and de-aerated by bubbling with nitrogen gas for 20–30 min before each experiment. The electrodeposition/stripping of lithium was performed in an argon glove box at 50 °C. 1 mm diameter nickel, glassy carbon and platinum working electrodes were used, with a lithium foil counter electrode and lithium quasi-reference electrode—this is only referred to as a pseudo reference since the actual redox couple cannot be rigorously identified; Lewandowski and Swiderska-Mocek have called this a Li/SEI/Li+ electrode,[8] however, the potentials are within ~20 mV for a range of cations with NTf_2. Lithium bis(trifluoromethanesulfonyl)amide was dissolved in $[P_{1\,2\,2\,4}][NTf_2]$ (0.2916 mol kg^{-1}) in an argon glove box and the mixture dried at 100 °C under vacuum for 24 h.

Synthesis

Materials. Sodium tetrafluoroborate, potassium hexafluorophosphate, sodium dicyanamide and potassium thiocyanate were purchased from Sigma-Aldrich and used as received. Lithium bis(trifluoromethanesulfonyl)amide was purchased from 3M, potassium bis(fluorosulfonyl)amide was purchased from Dai-chi Kogyo Seiyaku (Japan). Diethyl(methyl) isobutylphosphonium tosylate, triisobutyl(methyl)phosphonium tosylate, triethyl(methyl)phosphonium tosylate and triethyl(isobutyl)phosphonium tosylate were purchased from Cytec Industries and used as received.

Diethyl(methyl)(isobutyl)phosphonium bis(trifluoromethanesulfonyl)amide, $[P_{1\,2\,2\,4}][NTf_2]$. Diethyl(methyl)(isobutyl) phosphonium tosylate (20 g, 0.06 mol) and lithium bis(trifluoromethanesulfonyl)amide (18 g, 0.06 mol) were added together in water (100 mL) producing a white precipitate. The slurry was stirred overnight at room temperature before the solid was isolated by filtration and washed several times with water. The solid product was then dissolved in dichloromethane and the organic phase again washed with water. The dichloromethane was then removed on a rotary evaporator and the solid product was dried at 70 °C for 48 hours under vacuum. ^{1}H NMR (d_6-DMSO, 400 MHz) δ 1.02–1.04 ppm (3H, d, $J = 8$ Hz), 1.09–1.19 ppm (3H, m), 1.79–1.83 ppm (3H, d, $J = 13.6$ Hz), 1.96–2.08 ppm (1H, m), 2.12–2.25 ppm (2H, m). Mass spec: ES$^+$ *m/z* 161.1 $(C_9H_{22}P)^+$, ES$^-$ *m/z* $(NTf_2)^-$. Water content: 100 ppm.

Diethyl(methyl)(isobutyl)phosphonium bis(fluorosulfonyl)amide, $[P_{1\,2\,2\,4}][FSA]$. Diethyl(methyl)(isobutyl)phosphonium tosylate (10 g, 0.03 mol) and potassium bis(fluorosulfonyl)amide (7 g, 0.03 mol) were mixed together in water (50 mL), forming a clear liquid as a second phase. The two phases were separated and the ionic liquid phase was washed several times with distilled water and then dried *in vacuo* at 70 °C for several days. ^{1}H NMR (d_6-DMSO, 400 MHz) δ 1.02–1.04 ppm (3H, d, $J = 8$ Hz), 1.09–1.19 ppm (3H, m), 1.79–1.83 ppm (3H, d, $J = 13.6$ Hz), 1.96–2.08 ppm (1H, m), 2.12–2.25 ppm (2H, m). Mass spec: ES$^+$ *m/z* 161.1 $(C_9H_{22}P)^+$, ES$^-$ *m/z* 180 $(N(SO_2F)_2)^-$. Water content: 120 ppm.

Diethyl(methyl)(isobutyl)phosphonium hexafluorophosphate, $[P_{1\,2\,2\,4}][PF_6]$. Potassium hexafluorophosphate (11 g, 0.06 mol) was added to diethyl(methyl)(isobutyl)phosphonium tosylate (20 g, 0.06 mol) in distilled water, immediately forming the product as a white precipitate. The precipitate was isolated by filtration, washed several times with distilled water and dried *in vacuo* for several days at 100 °C. ^{1}H NMR (d_6-DMSO, 400 MHz) δ 1.02–1.04 ppm (3H, d, $J = 8$ Hz), 1.09–1.19 ppm (3H, m), 1.79–1.83 ppm (3H, d, $J = 13.6$ Hz), 1.96–2.08 ppm (1H, m), 2.12–2.25 ppm (2H, m). Mass spec: ES$^+$ *m/z* 161.1 $(C_9H_{22}P)^+$, ES$^-$ *m/z* 145 $(PF_6)^-$.

Diethyl(methyl)(isobutyl)phosphonium tetrafluoroborate, $[P_{1\,2\,2\,4}][BF_4]$. Sodium tetrafluoroborate (9 g, 0.08 mol) was added to diethyl(methyl)(isobutyl)phosphonium tosylate (25 g, 0.075 mol) in anhydrous acetone (100 mL) under a nitrogen atmosphere and the mixture refluxed overnight at 70 °C, producing a white precipitate (sodium tosylate). The precipitate was removed by filtration (200 nm filter) and the acetone removed under vacuum. The solid product was then recrystallised several times from acetone/dichloromethane. ^{1}H NMR (d_6-DMSO, 400 MHz) δ 1.02–1.04 ppm (3H, d, $J = 8$ Hz), 1.09–1.19 ppm (3H, m), 1.79–1.83 ppm (3H, d, $J = 13.6$ Hz), 1.96–2.08 ppm (1H, m), 2.12–2.25 ppm (2H, m). Mass spec: ES$^+$ *m/z* 161.1 $(C_9H_{22}P)^+$, ES$^-$ *m/z* 89.1 $(BF_4)^-$.

Diethyl(methyl)(isobutyl)phosphonium thiocyanate, $[P_{1\,2\,2\,4}][SCN]$. Potassium thiocyanate (3 g, 0.03 mol) was added to diethyl(methyl)(isobutyl)phosphonium tosylate (10 g, 0.03 mol) in anhydrous acetone (50 mL) and the mixture stirred at 70 °C for 3 days, forming a white precipitate (potassium tosylate). The precipitate was removed by filtration (200 nm filter) and the acetone removed under vacuum. The solid product was recrystallised several times from acetone/dichloromethane. ^{1}H NMR (d_6-DMSO, 400 MHz) δ 1.02–1.04 ppm (3H, d, $J = 8$ Hz), 1.09–1.19 ppm (3H, m), 1.79–1.83 ppm (3H, d, $J = 13.6$ Hz), 1.96–2.08 ppm (1H, m), 2.12–2.25 ppm (2H, m). Mass spec: ES$^+$ *m/z* 161.1 $(C_9H_{22}P)^+$, ES$^-$ *m/z* 58 $(SCN)^-$.

Diethyl(methyl)(isobutyl)phosphonium dicyanamide, $[P_{1\,2\,2\,4}][N(CN)_2]$. Sodium dicyanamide (3 g, 0.03 mol) was added to diethyl(methyl)(isobutyl)phosphonium tosylate (10 g, 0.03 mol) in anhydrous acetone (50 mL) and the mixture stirred at 70 °C overnight, forming a white precipitate (sodium tosylate). The white precipitate was removed by filtration (200 nm filter) and the acetone removed under vacuum. The liquid product was washed again with dry acetone and filtered to ensure that all of the sodium tosylate had been removed. ^{1}H NMR (d_6-DMSO, 400 MHz) δ 1.02–1.04 ppm (3H, d, $J = 8$ Hz), 1.09–1.19 ppm (3H, m), 1.79–1.83 ppm (3H, d, $J = 13.6$ Hz), 1.96–2.08 ppm (1H, m), 2.12–2.25 ppm (2H, m). Mass spec: ES$^+$ *m/z* 161.1 $(C_9H_{22}P)^+$, ES$^-$ *m/z* 66 $(N(CN)_2)^-$. Water content: 165 ppm.

Triisobutyl(methyl)phosphonium bis(trifluoromethanesulfonyl)amide, $[P_{1\,4\,4\,4}][NTf_2]$. Lithium bis(trifluoromethanesulfonyl)amide (15 g, 0.05 mol) was added to triisobutyl(methyl)phosphonium tosylate (20 g, 0.05 mol) in distilled water (50 mL) and the mixture stirred at room temperature for several hours, forming the product as a white precipitate. The product was isolated by filtration, washed several times with distilled water, recrystallised from dichloromethane and dried at 100 °C under vacuum for 48 hours. ^{1}H NMR (d_6-DMSO, 400 MHz) δ 0.99–1.05 ppm (3H, d, $J = 6.4$ Hz), 1.88–1.93 ppm (3H, d, $J = 13.6$ Hz), 2.00–2.09 ppm (1H, m, $J = 6.4$ Hz), 2.16–2.21 ppm (2H, d, $J = 13.6$ Hz). Mass spec: ES$^+$ *m/z* 217.2 $(C_{13}H_{30}P)^+$, ES$^-$ *m/z* 280 $(NTf_2)^-$.

Triisobutyl(methyl)phosphonium bis(fluorosulfonyl)amide, $[P_{1\,4\,4\,4}][FSA]$. Potassium bis(fluorosulfonyl)amide (6 g, 0.03 mol) was added to triisobutyl(methyl)phosphonium tosylate (10 g, 0.03 mol) in distilled water (50 mL) and the solution stirred at room temperature for several hours, forming the product as a white precipitate. The product was isolated by filtration, washed several times with distilled water, recrystallised from dichloromethane and dried at 70 °C *in vacuo* for 48 hours. ^{1}H NMR (d_6-DMSO, 400 MHz) δ 1.02–1.04 ppm (3H, d,

$J = 6.8$ Hz), 1.89–1.93 ppm (3H, d, $J = 13.6$ Hz), 2.00–2.07 ppm (1H, m, $J = 6.4$ Hz), 2.16–2.20 ppm (2H, d, $J = 13.6$ Hz). Mass spec: ES^+ *m/z* 217.2 $(C_{13}H_{30}P)^+$, ES^- *m/z* 180 $(N(SO_2F)_2)^-$.

Triisobutyl(methyl)phosphonium hexafluorophosphate, [P1444][PF6]. Potassium hexafluorophosphate (15 g, 0.082 mol) was added to triisobutyl(methyl)phosphonium tosylate (30 g, 0.08 mol) in distilled water (50 mL) and the solution stirred at room temperature for several hours, forming the product as a white precipitate. The product was isolated by filtration, washed several times with distilled water, recrystallised from dichloromethane and dried at 70 °C *in vacuo* for 48 hours. ^{1}H NMR (d_6-DMSO, 400 MHz) δ 1.03–1.05 ppm (3H, d, $J = 6.8$ Hz), 1.89–1.93 ppm (3H, d, $J = 13.6$ Hz), 2.00–2.06 ppm (1H, m, $J = 6.4$ Hz), 2.16–2.21 ppm (2H, d, $J = 13.6$ Hz). Mass spec: ES^+ *m/z* 217.2 $(C_{13}H_{30}P)^+$, ES^- *m/z* 145 $(PF_6)^-$.

Triisobutyl(methyl)phosphonium thiocyanate, [P1444][SCN]. Potassium thiocyanate (6 g, 0.06 mol) was added to triisobutyl(methyl)phosphonium tosylate (20 g, 0.05 mol) in dry acetone (100 mL) and the solution stirred at 50 °C for 2 days, producing a white precipitate (potassium tosylate). The white precipitate was removed by filtration (200 nm filter) and the acetone removed under vacuum. The solid product was recrystallised several times from dichloromethane and dried for 2 days at 100 °C under vacuum. ^{1}H NMR (d_6-DMSO, 400 MHz) δ 1.03–1.05 ppm (3H, d, $J = 6.8$ Hz), 1.89–1.93 ppm (3H, d, $J = 13.6$ Hz), 2.00–2.06 ppm (1H, m, $J = 6.4$ Hz), 2.16–2.21 ppm (2H, d, $J = 13.6$ Hz). Mass spec: ES^+ *m/z* 217.2 $(C_{13}H_{30}P)^+$, ES^- *m/z* 58 $(SCN)^-$.

Triisobutyl(methyl)phosphonium tetrafluoroborate, [P1444][BF4]. Sodium tetrafluoroborate (9 g, 0.083 mol) was added to triisobutyl(methyl)phosphonium tosylate (30 g, 0.08 mol) in distilled water (50 mL) and the solution stirred at room temperature for several hours, producing the product as a white precipitate. The product was isolated by filtration, washed several times with distilled water, recrystallised from dichloromethane and dried at 70 °C *in vacuo* for 48 hours. ^{1}H NMR (d_6-DMSO, 400 MHz) δ 1.03–1.05 ppm (3H, d, $J = 6.8$ Hz), 1.89–1.93 ppm (3H, d, $J = 13.6$ Hz), 2.00–2.06 ppm (1H, m, $J = 6.4$ Hz), 2.16–2.21 ppm (2H, d, $J = 13.6$ Hz). Mass spec: ES^+ *m/z* 217.2 $(C_{13}H_{30}P)^+$, ES^- *m/z* 87 $(BF_4)^-$.

Triethyl(methyl)phosphonium bis(trifluoromethanesulfonyl) amide, [P1222][NTf2]. Lithium bis(trifluoromethanesulfonyl) amide (8 g, 0.03 mol) was added to triethyl(methyl)phosphonium tosylate (10 g, 0.03 mol) in distilled water (50 mL) and the solution stirred at room temperature for several hours, producing the product as a white precipitate. The product was then isolated by filtration, washed several times with distilled water, recrystallised from dichloromethane and dried at 70 °C *in vacuo* for 48 hours. ^{1}H NMR (d_6-DMSO, 400 MHz) δ 1.09–1.17 ppm (3H, m), 1.75–1.78 ppm (3H, d, $J = 14$ Hz), 2.14–2.23 ppm (2H, m). Mass spec: ES^+ *m/z* 133.1 $(C_7H_{18}P)^+$, ES^- *m/z* 280 $(NTf_2)^-$.

Triethyl(methyl)phosphonium bis(fluorosulfonyl)amide, [P1222][FSA]. Potassium bis(fluorosulfonyl)amide (7.2 g, 0.033 mol) was added to triethyl(methyl)phosphonium tosylate (10 g, 0.033 mol) in distilled water (50 mL) and the solution stirred at room temperature for several hours, giving the product as a white precipitate. The product was isolated by filtration, washed several times with distilled water, recrystallised from dichloromethane and dried at 70 °C *in vacuo* for 48 hours. ^{1}H NMR (d_6-DMSO, 400 MHz) δ 1.09–1.17 ppm (3H, m), 1.75–1.78 ppm (3H, d, $J = 14$ Hz), 2.14–2.23 ppm (2H, m). Mass spec: ES^+ *m/z* 133.1 $(C_7H_{18}P)^+$, ES^- *m/z* 180 $(N(SO_2F)_2)^-$.

Triethyl(butyl)phosphonium bis(trifluoromethanesulfonyl) amide, [P2224][NTf2]. Lithium bis(trifluoromethanesulfonyl) amide (8 g, 0.03 mol) was added to triethyl(isobutyl)phosphonium tosylate (10 g, 0.03 mol) in distilled water (50 mL) and the solution stirred at room temperature for several hours, giving the product as a white precipitate. The product was isolated by filtration, washed several times with distilled water, recrystallised from dichloromethane and dried at 70 °C *in vacuo* for 48 hours. ^{1}H NMR (d_6-DMSO, 400 MHz) δ 1.09–1.11 ppm (3H, m), 0.99–1.03, (3H, t), 1.97–2.08 ppm (2H, m), 2.17–2.26 ppm (2H, m). Mass spec: ES^+ *m/z* 175 $(C_{10}H_{24}P)^+$, ES^- *m/z* 280 $(NTf_2)^-$.

Triethyl(butyl)phosphonium bis(fluorosulfonyl)amide, [P2224][FSA]. Potassium bis(fluorosulfonyl)amide (6.5 g, 0.03 mol) was added to triethyl(butyl)phosphonium tosylate (10 g, 0.033 mol) in distilled water (50 mL) and the solution stirred at room temperature for several hours, giving the product as a colourless liquid in a second phase. The product was separated and washed several times with distilled water before being dissolved in dichloromethane and filtered (200 nm filter) to remove any residual potassium salts present. The product was then dried at 70 °C *in vacuo* for 48 hours. ^{1}H NMR (d_6-DMSO, 400 MHz) δ 1.09–1.11 ppm (3H, m), 0.99–1.03, (3H, t), 1.97–2.08 ppm (2H, m), 2.17–2.26 ppm (2H, m). Mass spec: ES^+ *m/z* 175 $(C_{10}H_{24}P)^+$, ES^- *m/z* 180 $(N(SO_2F)_2)^-$.

Acknowledgements

The authors gratefully acknowledge funding from the Australian Research Council through its Centre of Excellence program, its Discovery program (DP0986205) and also for fellowship support for J. M. Pringle (QEII) and D. R. MacFarlane (Federation Fellow). D.V. thanks the DEEWR, Government of Australia for his 2009 Endeavour Research Fellowship and CSIR, Government of India for granting leave. DV also thanks DRM and MF for hosting him at Monash.

References

1 S. M. Zakeeruddin and M. Graetzel, *Adv. Funct. Mater.*, 2009, **19**, 2187.
2 M. Gorlov and L. Kloo, *Dalton Trans.*, 2008, 2655.
3 W. Lu, A. G. Fadeev, B. Qi, E. Smela, B. R. Mattes, J. Ding, G. M. Spinks, J. Mazurkiewicz, D. Zhou, G. G. Wallace, D. R. MacFarlane, S. A. Forsyth and M. Forsyth, *Science*, 2002, **297**, 983.
4 M. S. Cho, H. J. Seo, J. D. Nam, H. R. Choi, J. C. Koo and Y. Lee, *Smart Mater. Struct.*, 2007, **16**, S237.
5 C. Plesse, F. Vidal, H. Randriamahazaka, D. Teyssie and C. Chevrot, *Polymer*, 2005, **46**, 7771.
6 P. C. Howlett, D. R. MacFarlane and A. F. Hollenkamp, *Electrochem. Solid-State Lett.*, 2004, **7**, A97.

7 G. H. Lane, P. M. Bayley, B. R. Clare, A. S. Best, D. R. MacFarlane, M. Forsyth and A. F. Hollenkamp, *J. Phys. Chem. C*, 2010, **114**, 21775.
8 A. Lewandowski and A. Swiderska-Mocek, *J. Power Sources*, 2009, **194**, 601.
9 S. K. Martha, E. Markevich, V. Burgel, G. Salitra, E. Zinigrad, B. Markovsky, H. Sclar, Z. Pramovich, O. Heik, D. Aurbach, I. Exnar, H. Buqa, T. Drezen, G. Semrau, M. Schmidt, D. Kovacheva and N. Saliyski, *J. Power Sources*, 2009, **189**, 288.
10 H. Matsumoto, H. Sakaebe and K. Tatsumi, *J. Power Sources*, 2005, **146**, 45.
11 S. S. Y. Tan and D. R. MacFarlane, *Top. Curr. Chem.*, 2009, **290**, 311.
12 Ionic Liquids: Industrial Applications for Green Chemistry, (Proceedings of a Symposium held 1–5 April 2001 in San Diego, California), in *ACS Symp. Ser.*, ed. R. D. Rogers and K. R. Seddon, 2002, p. 818.
13 *Ionic Liquids in Synthesis*, ed. P. Wasserscheid and T. Welton, *2nd edn*, 2008, vol. 1.
14 H. Olivier-Bourbigou, L. Magna and D. Morvan, *Appl. Catal., A*, 2010, **373**, 1.
15 P. D. de Maria, *Angew. Chem., Int. Ed.*, 2008, **47**, 6960.
16 Y. Katayama, R. Fukui and T. Miura, *J. Electrochem. Soc.*, 2007, **154**, D534.
17 P.-Y. Chen and C. L. Hussey, *Electrochim. Acta*, 2006, **52**, 1857.
18 Z. Chen, M. L. Zhang, W. Han, Z. Y. Hou and Y. D. Yan, *J. Alloys Compd.*, 2008, **464**, 174.
19 W. Dobbs, J.-M. Suisse, L. Douce and R. Welter, *Angew. Chem., Int. Ed.*, 2006, **45**, 4179.
20 P. Bonhote, A.-P. Dias, N. Papageorgiou, K. Kalyanasundaram and M. Graetzel, *Inorg. Chem.*, 1996, **35**, 1168.
21 J. K. Ruff, *Inorg. Chem.*, 1965, **4**(10), 1446.
22 H. Matsumoto, H. Sakaebe, K. Tatsumi, M. Kikuta, E. Ishiko and M. Kono, *J. Power Sources*, 2006, **160**, 1308.
23 C. Michot, M. Armand, M. Gauthier and N. Ravet, Acep Inc., Can., Centre Nationalde la Recherche Scientifique, Universite de Montreal, Patent number WO 9940025, 1999, p. 43.
24 S. Tsuzuki, K. Hayamizu and S. Seki, *J. Phys. Chem. B*, 2010, **114**, 16329.
25 R. Vijayaraghavan, M. Surianarayanan, V. Armel, D. R. MacFarlane and V. P. Sridhar, *Chem. Commun.*, 2009, 6297.
26 S. A. Forsyth, J. M. Pringle and D. R. MacFarlane, *Aust. J. Chem.*, 2004, **57**, 113.
27 M. Freemantle, *An Introduction to Ionic Liquids*, 2010.
28 C. J. Bradaric, A. Downard, C. Kennedy, A. J. Robertson and Y. Zhou, *Green Chem.*, 2003, **5**, 143.
29 K. J. Fraser and D. R. MacFarlane, *Aust. J. Chem.*, 2009, **62**, 309.
30 C. Emnet, K. M. Weber, J. A. Vidal, C. S. Consorti, M. AlisonStuart and J. A. Gladysz, *Adv. Synth. Catal.*, 2006, **348**, 1625.
31 G. D. Yadav and S. P. Tekale, *Org. Process Res. Dev.*, 2010, **14**, 722.
32 E. Frackowiak, G. Lota and J. Pernak, *Appl. Phys. Lett.*, 2005, **86**, 164104.
33 R. E. Ramirez and E. M. Sanchez, *Sol. Energy Mater. Sol. Cells*, 2006, **90**, 2384.
34 Y. Kunugi, H. Hayakawa, K. Tsunashima and M. Sugiya, *Bull. Chem. Soc. Jpn.*, 2007, **80**, 2473.
35 R. E. Ramirez, L. C. Torres-Gonzalez and E. M. Sanchez, *J. Electrochem. Soc.*, 2007, **154**, B229.
36 V. Armel, J. M. Pringle, M. Forsyth, D. R. MacFarlane, D. L. Officer and P. Wagner, *Chem. Commun.*, 2010, **46**, 3146.
37 M. Forsyth, W. C. Neil, P. C. Howlett, D. R. MacFarlane, B. R. W. Hinton, N. Rocher, T. F. Kemp and M. E. Smith, *ACS Appl. Mater. Interfaces*, 2009, **1**, 1045.
38 P. C. Howlett, J. Efthimiadis, P. Hale, G. A. van Riessen, D. R. MacFarlane and M. Forsyth, *J. Electrochem. Soc.*, 2010, **157**, C392.
39 P. C. Howlett, S. Zhang, D. R. MacFarlane and M. Forsyth, *Aust. J. Chem.*, 2007, **60**, 43.
40 A. E. Somers, P. C. Howlett, J. Sun, D. R. MacFarlane and M. Forsyth, *Tribol. Lett.*, 2010, **40**, 279.
41 A. E. Somers, P. C. Howlett, J. Sun, D. R. MacFarlane and M. Forsyth, *WIT Trans. Eng. Sci.*, 2010, **66**, 273.
42 T. Ramnial, D. D. Ino and J. A. C. Clyburne, *Chem. Commun.*, 2005, 325.
43 T. Ramnial, S. A. Taylor, M. L. Bender, B. Gorodetsky, P. T. K. Lee, D. A. Dickie, B. M. McCollum, C. C. Pye, C. J. Walsby and J. A. C. Clyburne, *J. Org. Chem.*, 2008, **73**, 801.
44 M. Ishikawa, T. Sugimoto, M. Kikuta, E. Ishiko and M. Kono, *J. Power Sources*, 2006, **162**, 658.
45 K. Tsunashima, S. Kodama, M. Sugiya and Y. Kunugi, *Electrochim. Acta*, 2010, **56**, 762.
46 K. Tsunashima and M. Sugiya, *Electrochem. Commun.*, 2007, **9**, 2353.
47 K. Tsunashima and M. Sugiya, *Electrochem. Solid-State Lett.*, 2008, **11**, A17.
48 K. Tsunashima, F. Yonekawa and M. Sugiya, *Chem. Lett.*, 2008, **37**, 314.
49 J. A. Vega, J. Zhou and P. A. Kohl, *J. Electrochem. Soc.*, 2009, **156**, A253.
50 J. M. Pringle, P. C. Howlett, D. R. MacFarlane and M. Forsyth, *J. Mater. Chem.*, 2010, **20**, 2056.
51 P. C. Howlett, Y. Shekibi, D. R. MacFarlane and M. Forsyth, *Adv. Eng. Mater.*, 2009, **11**, 1044.
52 D. R. MacFarlane, J. Huang and M. Forsyth, *Nature*, 1999, **402**, 792.
53 K. R. Seddon, A. Stark and M.-J. Torres, *Pure Appl. Chem.*, 2000, **72**, 2275.
54 D. S. Silvester and R. G. Compton, *Z. Phys. Chem.*, 2006, **220**, 1247.
55 J. Timmermans, *Phys. Chem. Solids*, 1961, **18**, 1.
56 K. R. Seddon, *Nat. Mater.*, 2003, **2**, 363.
57 D. R. MacFarlane, P. Meakin, N. Amini and M. Forsyth, *J. Phys.: Condens. Matter*, 2001, **13**, 8257.
58 J. Huang and A. F. Hollenkamp, *J. Phys. Chem. C*, 2010, **114**, 21840.
59 J. Adebahr, J. Seeber Aaron, R. MacFarlane Douglas and M. Forsyth, *J Phys Chem B*, 2005, **109**, 20087.
60 D. R. MacFarlane and M. Forsyth, *Adv. Mater. (Weinheim, Ger.)*, 2001, **13**, 957.
61 W. Xu, E. I. Cooper and C. A. Angell, *J. Phys. Chem. B*, 2003, **107**, 6170.
62 M. Yoshizawa, W. Xu and C. A. Angell, *J. Am. Chem. Soc.*, 2003, **125**, 15411.
63 D. R. MacFarlane, M. Forsyth, E. I. Izgorodina, A. P. Abbott, G. Annat and K. Fraser, *Phys. Chem. Chem. Phys.*, 2009, **11**, 4962.
64 C. Zhao, G. Burrell, A. J. Torriero Angel, F. Separovic, F. Dunlop Noel, R. MacFarlane Douglas and M. Bond Alan, *J Phys Chem B*, 2008, **112**, 6923.
65 M. Galinski, A. Lewandowski and I. Stepniak, *Electrochim. Acta*, 2006, **51**, 5567.
66 H. Liu, Y. Liu and J. Li, *Phys. Chem. Chem. Phys.*, 2010, **12**, 1685.
67 K. Tsunashima, E. Niwa, S. Kodama, M. Sugiya and Y. Ono, *J. Phys. Chem. B*, 2009, **113**, 15870.
68 D. R. MacFarlane, P. Meakin, J. Sun, N. Amini and M. Forsyth, *J. Phys. Chem. B*, 1999, **103**, 4164.
69 S. Fang, L. Yang, J. Wang, H. Zhang, K. Tachibana and K. Kamijima, *J. Power Sources*, 2009, **191**, 619.
70 N. Byrne, P. C. Howlett, D. R. MacFarlane and M. Forsyth, *Adv. Mater.*, 2005, **17**, 2497.
71 D. Aurbach, *Nonaqueous Electrochemistry*, 1999.
72 P. C. Howlett, N. Brack, A. F. Hollenkamp, M. Forsyth and D. R. MacFarlane, *J. Electrochem. Soc.*, 2006, **153**, A595.
73 P. C. Howlett, E. I. Izgorodina, M. Forsyth and D. R. MacFarlane, *Z. Phys. Chem.*, 2006, **220**, 1483.
74 S. Randstroem, M. Montanino, G. B. Appetecchi, C. Lagergren, A. Moreno and S. Passerini, *Electrochim. Acta*, 2008, **53**, 6397.
75 R. Wibowo, S. E. Ward Jones and R. G. Compton, *J. Phys. Chem. B*, 2009, **113**, 12293.

